ORIGINAL PAPER

Sedimentation and Organic Carbon Burial in the Yangtze River and Hudson River Estuaries: Implications for the Global Carbon Budget

Jun Zhu · Curtis R. Olsen

Abstract   One of the most important challenges in global climate change research is balancing the carbon budget within the global carbon cycle. Carbon burial in sediments at the land–ocean interface has been difficult to quantify and model because it represents non-steady-state boundary conditions that are also affected by human activities. In this study, we document carbon burial rates in the Yangtze River ($1.6–4.9 \times 10^{12}$ gC year^{-1}) and Hudson River ($1.8–3.6 \times 10^{10}$ gC year^{-1}) estuaries and integrate our results with carbon burial rates determined by others in the world's 25 largest river-estuarine systems ($6–11 \times 10^{13}$ gC year^{-1}). Our results indicate that carbon burial in estuaries, bays, coves, lagoons, mud flats, marshes, mangroves, and other highly productive or protected low-energy areas at the land–ocean interface along the entirety of the world's coastlines may serve as an unrecognized sink within the global carbon budget.

Keywords   Estuaries · Sediment accumulation · Organic carbon burial · Land–ocean interface · Global carbon budget

1 Introduction

For more than three decades, scientists examining the global carbon cycle have been looking for a missing carbon sink of ~ 2 PgC year^{-1} to balance the global carbon budget (Bolin 1977; Broecker et al. 1979). For the past two decades, this missing carbon sink has increased to ~ 3 PgC year^{-1}, and it has also been referred to as a "land sink" (Canadell et al. 2007) or "residual terrestrial sink" (Houghton and Goodale 2004; Prentice et al. 2001). In this study, we used geographic information systems (GIS) and radionuclide

J. Zhu (✉)
Bren School of Environmental Science and Management, University of California Santa Barbara, 2400 Bren Hall, Santa Barbara, CA 93106-5131, USA
e-mail: jzhu@bren.ucsb.edu

C. R. Olsen
Department of Environmental, Earth and Ocean Sciences, University of Massachusetts Boston, 100 Morrissey Boulevard, Boston, MA 02125-3393, USA

dating techniques (^{137}Cs) to examine sediment accumulation and to estimate carbon burial in both the Yangtze River and the Hudson River estuaries over the past 50 years. The Yangtze River estuary represents large river-estuarine–deltaic systems, which rapidly trap and bury carbon in sediments at the land–ocean interface. Geologists search for ancient deltaic areas in the geologic record because over time, this buried carbon forms oil. The medium-sized Hudson River estuary also effectively traps waterborne carbon and sediment due to its estuarine circulation pattern. This circulation pattern is characterized by a net seaward flow at the ocean surface and a net landward flow along the ocean bottom. As a result, the carbon produced in the shelf waters often sinks to the bottom and is thus transported landward across the shelf to accumulate in the marshes, mudflats, bays, and estuaries at the land–ocean interface. In this study, we have also integrated our results with those of others who have examined carbon burial in various estuarine systems worldwide to evaluate the importance of carbon burial at the land–ocean interface within the global carbon cycle.

As ephemeral non-steady-state features, estuaries and other coastal marginal areas are formed at the land–ocean interface during interglacial periods of ice melting and sea-level rise. Our present interglacial period started ∼18,000 years ago, during which sea level has risen ∼120 m to cover the world's continental shelves, flood coastal lands, and submerge ancient Greek and Roman cities (Fairbridge 1961). During past glacial times when sea level was much lower, major rivers discharged particles coated with carbon films (Mayer 1994), nutrients, and particulate organic carbon (POC) directly into the deep ocean, forming channels on continental shelves and canyons on continental slopes (Broecker 2003). During interglacial times, however, carbon-coated particles and POC are effectively trapped within the land–ocean interface. This trapping results from an estuarine circulation pattern that is governed by external forces (gravity, tides, and winds), internal forces (temperature and salinity pressure gradients), and the *Coriolis* Effect and is characterized by a net seaward flow of fresher water at the surface and a net landward flow of more saline water along the bottom (Fig. 1). This net landward flow along the bottom extends from across the continental shelf to the tip of salt water penetration in river-estuarine systems (Biscaye 1994), where iron and dissolved organic carbon (DOC) flocculates along with carbon-coated particles, POC, and resuspended sediments to form a zone of turbidity maximum (Schubel 1968; Sholkovitz 1976) and a zone of rapid sediment and carbon accumulation.

Many large estuaries, like Chesapeake Bay, have multiple deltas, one forming at its mouth and building landward due to sandy sediments supplied by longshore and across-shelf transport, and several other deltas forming at the mouths of its tributary rivers, due to the flocculation and deposition of finer-grained sediments (Donoghue et al. 1989). In the Savannah River estuary, Olsen et al. (1989) showed that riverborne particles had a distinctly different ^{238}Pu/^{239,240}Pu ratio compared to the global fallout plutonium ratio measured on oceanic particles. They used this difference to document that riverborne particles were primarily deposited in upstream areas of the Savannah River near its estuarine turbidity maximum and that the sediments rapidly accumulating in the estuary and in Savannah Harbor were marine particles that were transported along shore and landward across the shelf or produced in situ within the estuary. Mulholland and Olsen (1992) used stable isotope ratios of carbon, nitrogen, and sulfur to determine the source functions for organic carbon in the Savannah River estuary. Their results indicated that over 74 % of the organic particles in suspension or on the bottom of the estuary were of marine origin and that ∼22 % of the organic material (in bottom sediments) near the tip of salt water penetration was also of marine or estuarine origin. Therefore, particles, carbon,
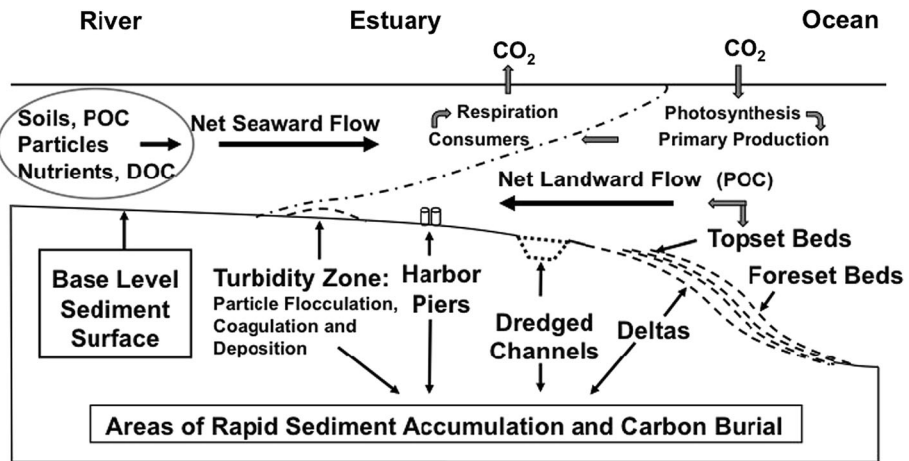
River **Estuary** **Ocean**

CO$_2$ CO$_2$

Soils, POC Particles Nutrients, DOC

Net Seaward Flow

Respiration Consumers

Photosynthesis Primary Production

Net Landward Flow (POC)

Base Level Sediment Surface

Turbidity Zone: Particle Flocculation, Coagulation and Deposition

Harbor Piers

Dredged Channels

Deltas

Topset Beds

Foreset Beds

Areas of Rapid Sediment Accumulation and Carbon Burial

Fig. 1 Schematic drawing of net estuarine circulation at the land–ocean interface indicating that particles and carbon from riverine, marginal, and marine sources are effectively trapped at the land–ocean interface

and particle-reactive contaminants transported from watersheds, introduced via municipal wastewater inputs, produced in situ, or transported landward from marine sources are effectively being trapped at the land–ocean interface due to a rising sea level during our current interglacial period. Today, oil and gas companies use seismic profiling and other geophysical methods to search for ancient estuaries, bays, and deltas in the geologic record as source rocks for hydrocarbons.

Although differences in the biological, chemical, geological, and hydrological characteristics cause patterns of sediment accumulation and carbon burial to be complex and unique within each estuarine system (Wright 1989), there appear to be certain generic features that are common to all. Using the established geological concept of "an equilibrium profile," Olsen et al. (1993)documented that the accumulation of particles and organic carbon tends to be negligible (0–5 mm year^{-1}) in estuarine and coastal areas, where the sediment surface has reached a state of "dynamic equilibrium" with its present-day hydraulic regime. These areas generally occur naturally in river channels, on subtidal banks, and on continental shelves (Type I Areas in Fig. 2). The suspended particulate load tends to bypass these "equilibrium-surface" areas through a series of deposition and resuspension events to accumulate at moderate rates (1–5 cm year^{-1}) in protected areas, such as marginal coves (Type II Areas in Fig. 2), or at extremely rapid rates (5–100 cm year^{-1}) in "non-equilibrium" areas (Type III Areas in Fig. 2), where the sediment surface is temporally out of equilibrium with its physical regime. As illustrated in Figs. 1 and 2, these "non-equilibrium areas" of rapid sediment accumulation and carbon burial can occur naturally in river-estuarine systems, such as around the turbidity maxima, in protected marginal areas, in deltaic environments, or in areas affected by human activities, such as dredged channels, harbor slips, piers, bridges, dams, or other structures affecting the physical regime (Schubel and Meade 1977; Smith 2007; Zhu 2010).

Scientists throughout the world have been examining the physics and biogeochemistry of estuaries and using carbon to understand, quantify, and model ecological dynamics at the land–ocean interface (Aller et al. 2008; Berner 1982; Benner et al. 2004; Bianchi and Allison 2009; Dürr et al. 2011; McKee et al. 2004). Within the global carbon cycle, the
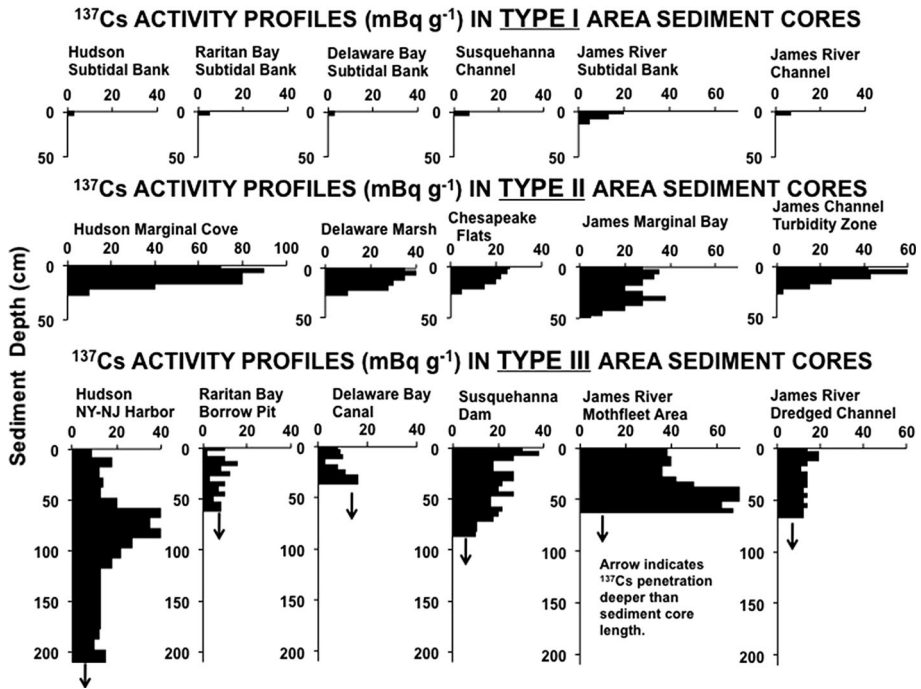
Fig. 2 Vertical profiles of cesium-137 (half-life = 30 years) in sediment cores collected in estuaries along the east coast of the United States generally fall into three distinct types. These three types reflect the extent to which the estuarine sediment surface has attained equilibrium with its present wave, current, flow, and sea-level regime. This figure was modified from Olsen et al. (1993)

importance of the estuarine water column as a source for CO_2 to the atmosphere has been well documented (Cai et al. 2006; Fagan and Mackenzie 2007; Green et al. 2006).The importance of carbon burial at the land–ocean interface as a sink for atmospheric CO_2 within the global carbon cycle has been difficult to evaluate, because (1) estuaries are ephemeral non-steady-state features that form at the land–ocean interface during inter-glacial warming periods, which complicates boundary-condition considerations in mod-eling carbon source and sink functions; (2) sediment and carbon accumulation patterns are affected simultaneously by both short-term processes (tides, waves, storms, and seasonal changes in freshwater discharge) and long-term processes in association with sea-level rise; and (3) estuaries often experience non-steady-state conditions associated with increasing human population, nutrient supply, and urbanization.

2 Study Areas

2.1 Yangtze River Estuary

The Yangtze River is the largest river in China, draining an area of $\sim 1.8 \times 10^6$ km^2 (~ 20 % of the mainland). On a global basis, the Yangtze River ranks fifth for freshwater discharge and fourth for sediment load (Eisma 1998). Annual freshwater discharge and sediment load averaged about 9.0×10^{11} m^3 year^{-1} and 4.3×10^8 mt year^{-1},

respectively, from 1951 to 2000, as gauged at Datong Station located $\sim$600 km upstream from the Yangtze River mouth. The Yangtze River mouth at the land–ocean interface is presently 120 km long and 90 km wide at its outer limit, where the river is bifurcated into the North and South Branches at the Chongming Island, split into the North and South Channels in the South Branch by Changxing and Hengsha Islands, and finally branched into the North and South Passages by the Jiuduansha Shoal (Fig. 3). Tidal height averages 2–3 m with a maximum height of 6 m (Yang 1999).

The deposition of sediments in the Yangtze River estuary and delta has resulted in the formation of land, averaging $\sim$5 km^2 year^{-1} over the last 2,000 years (Yang et al. 2001). Presently, over 98 % of the riverine discharge flows through the South Branch (Fig. 3), and as a result, the South Branch outlets are currently the major deltaic depocenters for riverine sediments (Yang et al. 2003). Approximately half of the riverine sediments is retained within the estuary and the other half is discharged onto the shelf and transported along the southeast coast of China by alongshore currents (Yang et al. 2000). As illustrated in Fig. 3, this study examines sediment accumulation in tidal flat areas (east of the Chongming, Changxing, Hengsha, and Jiuduansha Islands), in deltaic topset bed area (east of the Jiuduansha Shoal), and along a 60 km transect across the topset and foreset beds of the Yangtze River delta. The estimate of organic carbon burial (based on sediment accumulation rate) was confined within a 2,500 km^2 area.
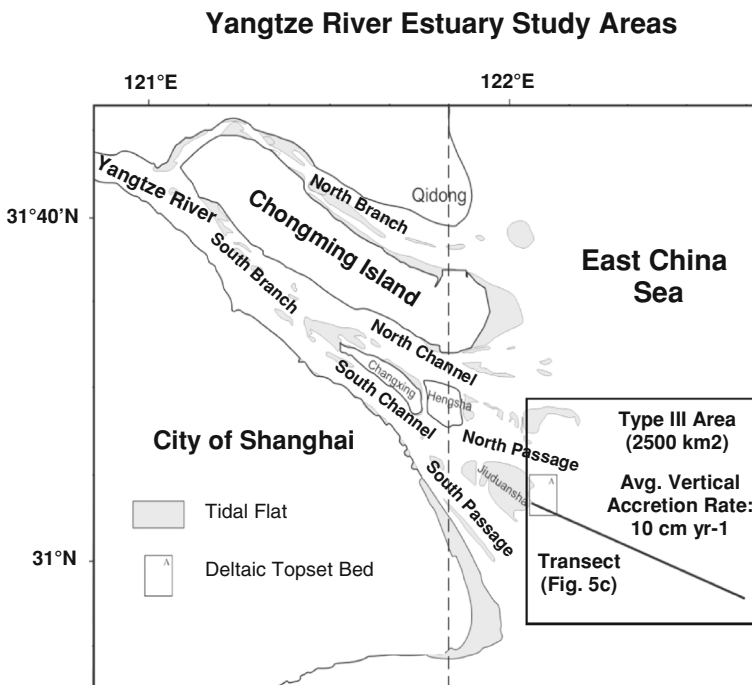

Fig. 3 Map of the Yangtze River estuary illustrating its tidal flat areas, as well as its deltaic topset and foreset-bed areas. The tidal flat study areas are the *shaded areas* located east of the 121°50′E line of latitude. The deltaic topset bed study area is located east of the Jiuduansha Shoal (*small-boxed area* A). The *larger box* covers a 2,500 km^2 Type III area, which encompasses both the topset and the foreset beds of the Yangtze River delta. The *line* within the *larger box* illustrates our deltaic transect

2.2 Hudson River Estuary

The Hudson River estuary is one of the most urbanized and industrialized estuaries on the east coast of the United States, draining an area of $\sim 3.5 \times 10^4$ km². Mean monthly freshwater discharge past the southern tip of the Manhattan Island (Fig. 4) ranges from 150 to 250 m³ s⁻¹ during low-flow conditions in the summer to as high as 1,000–1,500 m³ s⁻¹ during the spring freshet (Chillrud 1996). Annual freshwater flow averaged $\sim 1.7 \times 10^{10}$ m³. Mean tidal flow varies from 3,000 to 10,000 m³ s⁻¹ with maximum tidal current velocities of ~ 1 m s⁻¹. As a partially mixed estuary, an estuarine turbidity maximum (ETM) forms and its position fluctuates with freshwater discharge. During low freshwater flow conditions, the ETM can reach as far as ~ 60 km upstream of the Battery (Geyer et al. 2001). During high freshwater flow conditions, the ETM can penetrate as far downstream as the George Washington Bridge, ~ 18 km upstream of the Battery (Woodruff et al. 2001). Mean annual suspended sediment load from the freshwater reach of the estuary is 737,000 mt (Wall et al., 2008). The Hudson River estuary also receives ~ 100 m³ s⁻¹ of wastewater from sewage treatment facilities, as well as discharges from about 400 industrial sources and 700 combined storm water and untreated sewage outfalls (CSOs). Wastewater can account for as much as 40 % of the freshwater flow during low-flow conditions, and ~ 90 % of the wastewater discharge occurs in the lower 30 km of the estuary (Sanudo-Wilhelmy and Gill 1999).

In this study, the lower Hudson River estuary is defined as the area extending from its mouth at the Narrows to the George Washington Bridge (Fig. 4). Previous studies have indicated that the riverine suspended particulate load undergoes a series of deposition and
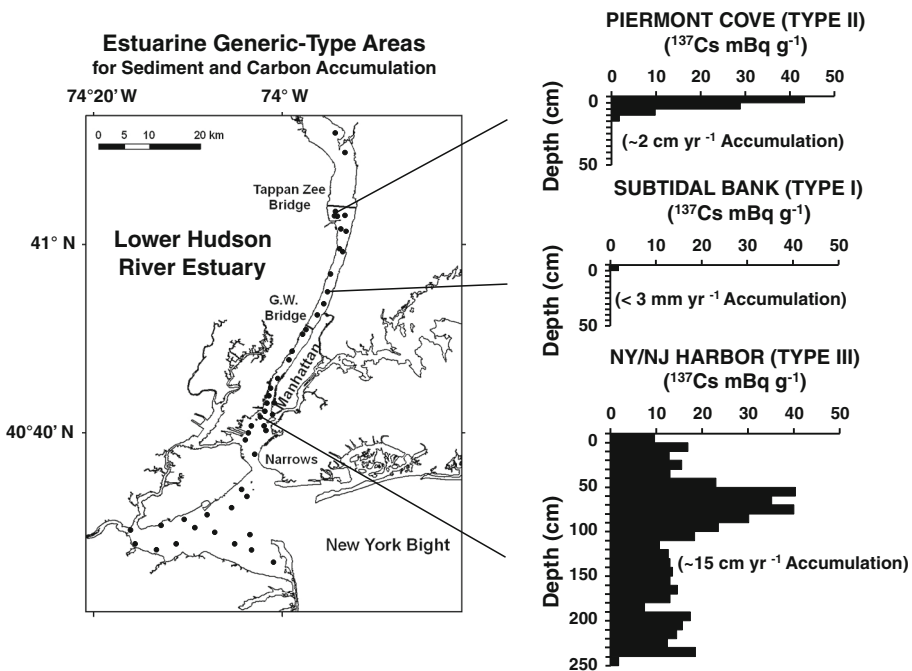

Fig. 4 Map of the lower Hudson River estuary identifying sediment core locations and illustrating the ¹³⁷Cs vertical profiles representing the three estuarine generic-type areas for sediment and carbon accumulation

resuspension events to ultimately accumulate at extremely rapid rates (5–20 cm year^{-1}) in the dredged channels, abandoned harbor slips, and other low-energy areas in the lower Hudson River estuary (Bopp et al. 1993; Smith 2007; Zhu 2010).

3 Sites and Methodology

3.1 Hudson River Estuary

3.1.1 Sediment Sampling

This study used data obtained from more than 80 sediment cores collected in the Hudson River estuary from the early 1970s to 2007 (Fig. 4). Short sediment cores, ranging from 50 to 100 cm in length, were collected using a gravity coring device, and longer sediment cores, ranging up to 250 cm, were collected using vibra- or piston-corers. All the sediment cores were extruded, described, and sectioned within 24 h of collection. The sediment samples were weighed and dried in an oven at 50 °C over 24 h, weighed again, ground uniformly using a mortar and pestle, placed in plastic-lined aluminum cans, and analyzed for gamma-emitting radionuclides and sediment total organic carbon content (TOC$_{sed}$). Sediment water content is determined by using a function of pore water/bottom water ratio and (wet weight-dry weight)/wet weight ratio.

3.1.2 Gamma Spectrometric Analysis

All sediment radionuclide activities were determined by nondestructive gamma spectrometry. Most recently, these analyses were conducted using an ultra low-background, high-resolution Canberra (Be5030) Broad Energy Germanium planar detector, equipped with a Genie 2000 MCA (Canberra) microprocessor and an interactive peak-fit software package. The measured vertical distribution of cesium-137 (^{137}Cs, half-life = 30 years) in sediment cores was used to evaluate the rates of sediment and carbon accumulation in the lower Hudson River estuary. Most of the ^{137}Cs delivered to the Hudson River watershed occurred via global fallout from nuclear weapons testing starting in the later 1940s, which exhibited a peak in 1963. In addition, there was a significant coolant water release of ^{137}Cs in 1971 from the Indian Point Nuclear Power Plant (Buchanan, NY) that also served as a sediment stratigraphic marker for dating purposes (Chillrud 1996).

3.1.3 Carbon–Hydrogen–Nitrogen (CHN) Analysis

Sediment total organic carbon content (TOC$_{sed}$) was determined using loss-on-ignition for samples collected in the 1970s, and a Perkin-Elmer 2400 Carbon, Hydrogen, and Nitrogen (CHN) analyzer was used for more recent samples. The loss-on-ignition method estimated organic matter concentration by the weight loss-on-ignition at 375 °C for samples taken on precombusted and preweighed glass-fiber filters (GFC, 1.0 micron pore size).The CHN-analyzed sediment samples were acidified using 2–5 ml of 1 N HCl and then dried for 24–48 h at 60 °C to remove the inorganic fraction of carbon in the sediments. The CHN analyzer was calibrated using Acetanilide (71 % C and 10 % N) as the standards. Errors in the measured TOC$_{sed}$ values were calculated using the standard deviation of the measured standard values.

3.1.4 Bathymetric Change Analysis

Sediment accumulation patterns in the lower Hudson River estuary were also determined by comparing changes in bathymetry between 1930 and 2001, using two sets of navigational charts (sounding images) obtained from U.S. National Oceanic and Atmospheric Administration (NOAA).The navigational charts were geo-referenced to the same geographic coordinate system using ERDAS IMAGINE 9.1 software and then digitized using ESRI ArcGIS 9.2 software, to obtain the bathymetric information. These navigational charts covered our entire study area and were used to estimate sediment accumulation rates in the lower Hudson River estuary over the same time frame covered by our ^{137}Cs dating technique.

3.2 Yangtze River Estuary

A total of 19 navigational charts of the Yangtze River estuary from 1958 to 2001 were obtained from the Shanghai Sea Route and China Maritime Survey Bureaus to conduct bathymetric change analysis. These navigational charts spanning different time periods were digitized using MapInfo 6, processed using Surfer 3 and overlaid one another to determine the sediment accumulation rates on the tidal flat, on the deltaic topset bed, and along the transect over time. The sediment total organic carbon content (TOC_{sed}) in the Yangtze River estuary has been reported by others, ranging from 0.5 to 1.5 % (Lu et al. 2006; Wu et al. 2007).

4 Results and Discussion

4.1 Sediment Accumulation in the Yangtze River Estuary

Results from bathymetric change analysis described above indicate that sediments have been rapidly accumulating both laterally (progradation) and vertically (accretion) in the Yangtze River estuary over the last 40 years (Fig. 5). The growth rates of tidal flat surface areas have ranged from $\sim$3 to 13 km^2 year^{-1} (Fig. 5a). The sediment accumulation rate of the deltaic topset bed ranged from 5 to 20 cm year^{-1} (Fig. 5b). Vertical sediment accretion rates across the deltaic topset and foreset beds ranged from 5 to 20 cm year^{-1}, and the horizontal progradation of the entire Yangtze River delta varied from 6 to 12 km between 1958 and 1998 (Fig. 5c).

The data illustrated in Fig. 5 also indicate a decreasing trend in the rates of tidal flat growth and deltaic topset bed accretion. This decreasing trend probably reflects a reduction in the sediment load delivered to the Yangtze River estuary over the past 50 years. Previous research by Zhu (2003) documented that the sediment load at Datong Gauging station decreased by $\sim$25 % from 1951 to 2000 (Fig. 5d). Zhu (2003) also showed that a strong linear correlation ($R^2 = 0.8$ and $P < 0.01$) existed between the sediment load delivered to the East China Sea and the accretion rate of deltaic topset bed within the Yangtze River estuary. Previous research by Yang et al. (2005) also documented response of delta intertidal wetlands to decrease in riverine sediment supply. They suggested that when the deposition rate is higher than sinking rate (compaction rate + subsidence rate), it leads to increase in intertidal wetland elevation, which is in line with results from this study. Despite the decreasing trend in the riverine sediment loads to the estuary over the past 50 years (Fig. 5d), our results indicate that the average sediment accumulation rate
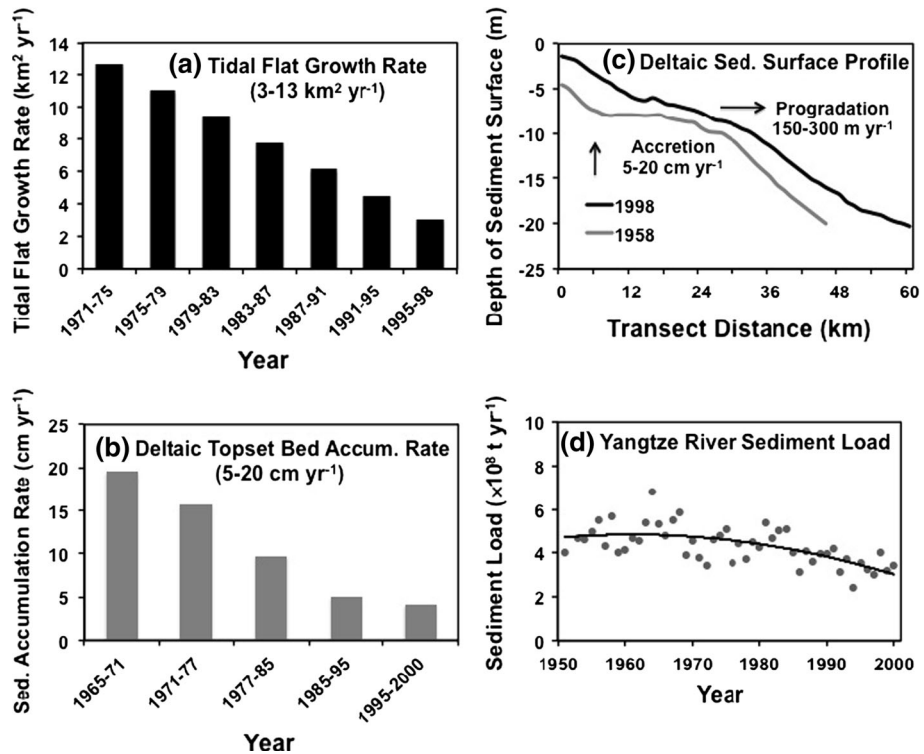
Fig. 5 Illustrations documenting changes in **a** Yangtze River tidal flat growth rates, **b** deltaic topset bed accumulation rates, **c** deltaic sediment surface elevation and foreset-bed progradation rates, and **d** changes in the riverine sediment load. These illustrations indicate rapid sediment accumulation, both vertically and laterally, in the Yangtze River estuary over a 40-year time period (1958–1998) and a decreasing trend in the riverine sediment load delivered to the estuary from 1951 to 2000

($\sim$10 cm year^{-1}) is still very high. Although there were upstream agriculture and levee developments during 1951–2000 (Yang et al. 2004), there were no dredging activities in the North Passage area of the Yangtze River estuary (Fig. 3), and the Three Gorges Dam was not yet constructed. As a result, sediment accumulation during our time period of study primarily reflected natural processes. Therefore, results from this study may provide baseline information that can be used to assess the impacts of urbanization and anthropogenic activities, such as large-dam construction and harbor dredging, on sediment dynamics and accumulation patterns within the Yangtze River estuary. Previous studies by Yang et al. (2005) and Zhu (2006) have shown that the construction of the Three Gorges Dam in 2001 significantly decreased the riverine sediment supply to the Yangtze River estuary.

4.2 Sediment Accumulation in the Lower Hudson River Estuary

Sediment accumulation patterns and rates were, respectively, determined in the lower Hudson River estuary, over a 70-year time frame using bathymetric change analysis (Fig. 6) and radionuclide dating techniques (Fig. 7). Figure 6 was made based on the changes in bathymetry over time, indicating sediment accumulation (shoaling) and erosion

(deepening). Channel deepening could be due to sediment erosion or human activities, such as dredging. Dredging creates temporary sediment accommodation space, which leads to sediment accumulation. Therefore, the actual long-term deepening is likely due to sediment erosion. Figure 7 shows cesium-137 and organic carbon vertical profiles in two sediments cores collected in two locations, representing two types of sedimentation regimes. As indicated in Figs. 6 and 7, the areas of sediment accumulation determined by bathymetric change analysis often coincided with the "non-equilibrium areas" that were determined by the ^{137}Cs sediment-depth profiles.

Previous studies have shown that $\sim 1.6 \times 10^6$ mt of fine-grained sediments are annually accumulating in the lower Hudson River estuary (Bokuniewicz and Ellsworth 1986; Chillrud 1996). Ellsworth (1986) estimated that system-wide accumulation is $0.5–5 \times 10^5$ mt year^{-1} greater than the sediment input from the riverine and marine sources. This deficit could potentially be balanced by bottom erosion 4.4×10^5 mt year^{-1} (Klingbeil and Sommerfield 2005). Olsen et al. (1984) quantified the source functions for this total annual sediment input using cesium and plutonium isotopic tracers. Their results indicated that $\sim 1.1 \pm 0.3 \times 10^6$ mt year^{-1} of fine-grained sediments were derived from
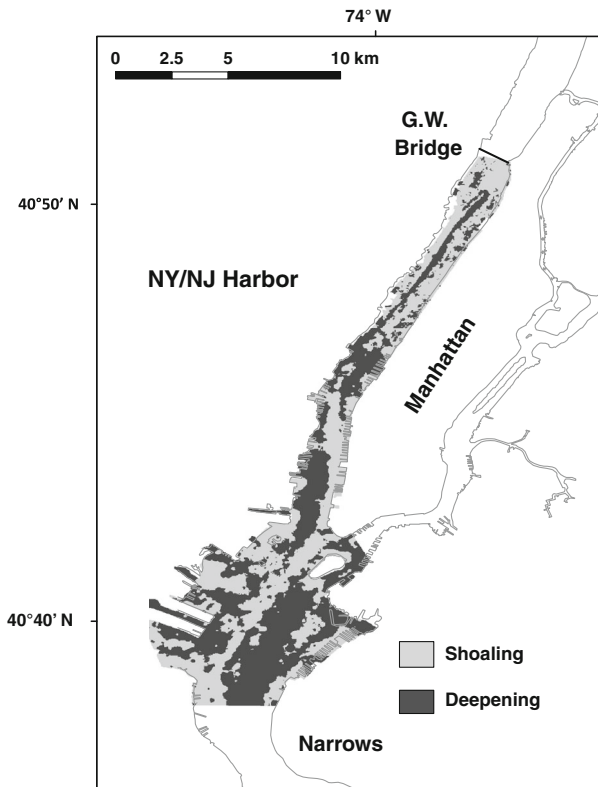

Fig. 6 Map of the New York/New Jersey Harbor (within the lower Hudson River estuary) illustrating changes in the sediment surface (shoaling or deepening) over a 70-year time span. In this urbanized estuary, dredging activities create a sediment surface far below its equilibrium depth, causing rapid sediment accumulation and carbon burial. As a result, the amount of sediment accumulating in the estuarine channel is balanced by the amount of sediment that is annually dredged from the channel ($\sim 1 \times 10^6$ mt year^{-1})
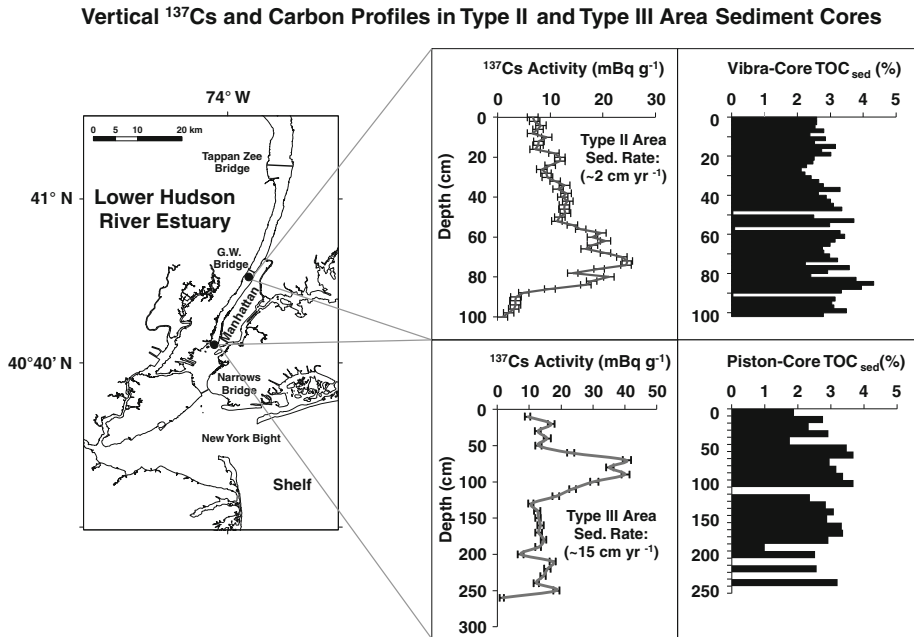
Vertical ^{137}Cs and Carbon Profiles in Type II and Type III Area Sediment Cores

Fig. 7 Vertical distributions of ^{137}Cs and sediment organic carbon content (TOC$_{sed}$) in a sediment piston-core (collected during 1975 in a previously dredged channel) and in a sediment vibra-core (collected during 2007 in a protected marginal cove). The large ^{137}Cs activity peak observed in both sediment cores was associated with a major coolant water release from the Indian Point Nuclear Power Facility in 1971

riverborne sources; $\sim 0.15 \pm 0.1 \times 10^6$ mt year^{-1} were derived from sewage solid inputs and in situ primary production; and $\sim 0.35 \pm 0.35 \times 10^6$ mt year^{-1} were transported landward into the estuary from marine sources. Records from the U.S. Army Corps of Engineers indicate that $\sim 1 \times 10^6$ mt of sediment were annually dredged from the main harbor channels to maintain "steady-state" navigable harbor depths (Panuzio 1965). If we assume that the remaining $\sim 0.6 \times 10^6$ mt of the total sediment input (1.6×10^6 mt) are accumulating in non-dredged areas of the lower Hudson River estuary, then the, nonet sediment accumulation has been balanced by channel dredging activities over the past 70 yrs as determined by our bathymetric change analysis in the main channel. The organic-rich and highly contaminated dredged spoils were previously dumped onto the continental shelf. Due to the landward transport of dredged spoils across the shelf bottom and their subsequent accumulation in protected areas onshore, these dredged spoils are no longer discharged offshore and are now used for landfill (Swanson et al. 2004).

The vertical profiles of ^{137}Cs and TOC$_{sed}$ for two selected sediment cores are illustrated and described in Fig. 7. Both sediment cores exhibit a large peak in ^{137}Cs, which was associated with a major release of coolant water in 1971 from the Indian Point Nuclear Power Plant (Buchanan, NY). Correlation of this 1971 reactor peak with the vertical distribution of ^{137}Cs in the sediments of the piston-core collected in 1975 indicated an average sediment accumulation rate of ~ 15 cm year^{-1} in the previously dredged channel. The vertical distribution of TOC in the sediments of the 1975 piston-core ranges from 2 to 4 %. Correlation of the 1971 reactor peak with the vertical distribution of ^{137}Cs in the sediments of the vibra-core collected in 2007 indicated an average sediment accumulation

rate of ~ 2 cm year^{-1} in the protected marginal cove near the George Washington Bridge. The global ^{137}Cs peak was not observed in either of the two sediment cores likely due to mixing. The vertical distribution of TOC in the sediments of the 2007 vibra-core also ranges from 2 to 4 %. The ^{137}Cs peak in both cores did not reflect changes in sediment grain size or composition as indicated by the measured vertical distribution of ^{40}K (half-life $= 1.27 \times 10^9$ years). Although the ^{40}K data are not presented in Fig. 7, previous work by Olsen (1979) has shown that ^{40}K is a good indicator of sediment grain size and composition (i.e., quartz-rich sandy sediments are characterized by low ^{40}K activities).

4.3 Sediment Organic Carbon Burial in the Yangtze River Estuary and the Hudson River Estuary

Sediment organic carbon burial (C_{Burial}) in both the Yangtze River and the Hudson River estuaries is a function of area (A), sediment accumulation rate (SAR), sediment bulk density (SBD), sediment total organic carbon content (TOC$_{\text{sed}}$), and its sediment burial efficiency(SBE).

$$C_{\text{Burial}} = A \times \text{SAR} \times \text{SBD} \times \text{TOC}_{\text{sed}} \times \text{SBE}$$

The sediment carbon burial efficiency (SBE) is the only unknown parameter in the above equation that is needed to calculate total organic carbon burial (C_{Burial}) in the sediments for both the Hudson and the Yangtze River estuaries. Because of the uncertainties associated with carbon remineralization and burial rates, we decided to use a sediment carbon burial efficiency of 100 % for Type III areas where sediment accumulation and carbon burial are >5 cm year^{-1}, as supported by our results in the Hudson River estuary and by other studies in the Yangtze River estuary, such as Lu et al. (2006). For Type II areas (marginal coves, with sediment accumulation rates of 1–5 cm year^{-1}), we also used a carbon burial efficiency of 100 %, which is also supported by our results in the Hudson River estuary. For Type I areas (in equilibrium with sea-level rise), we expect that the only carbon buried in these dynamic resuspension environments would be carbon trapped in the pores of mineral grains, where it is unavailable for remineralization (Mayer and Johnson 1994).

In the Yangtze River estuary, our study area encompassed the deltaic topset and foreset beds (see large box in Fig. 3), which also represented Type III areas. As a result, we expect that ~ 100 % of the carbon deposited on the Yangtze River delta is also retained in the sediments, which is supported by Lu et al. (2006), who showed no appreciable loss of organic carbon with depth in the sediment cores that they collected in the Yangtze River estuary. To calculate the total organic carbon burial (C_{Burial}) in the Yangtze River estuary, we used the following parameters: a Type III area (A) of 2,500 km^2; an average sediment accumulation rate (SAR) of 10 cm year^{-1}, an average of sedimentation rates on the deltaic topset bed and along the transect (Fig. 3); a sediment bulk density (SBD) of 1.3 g cm^{-3} (Yang et al. 2001); a range of sediment organic carbon content (TOC$_{\text{sed}}$) of 0.5–1.5 % (Lu et al. 2006; Wu et al. 2007; Zhu et al. 2006); and a sediment carbon burial efficiency (SBE) of 100 %.This calculation indicates that the total organic carbon burial in non-equilibrium Type III areas of the Yangtze River estuary and delta (2,500 km^2) ranged from 1.6 to 4.9×10^{12} gC year^{-1}. The total organic carbon burial rate over the entire East China Sea Shelf including the Yangtze River estuary and delta was 7.4×10^{12} gC year^{-1}, as determined by Deng et al. (2006). As a result, it appears that the total organic carbon burial in our small study area at the river mouth could account for as much as 66 % of the total organic carbon buried on the entire East China Sea Shelf.

In the Hudson River estuary, it appears that ~100 % of the organic carbon deposited is retained within the sediments of Type II (1–5 cm year^{-1}) and Type III (5–20 cm year^{-1}) areas, which is supported by the no appreciable loss of organic carbon with sediment depth (see Fig. 7). The observed variations of organic carbon in these sediment cores were primarily associated with changes in sediment grain size. To calculate the total organic carbon burial (C_{Burial}) in the lower Hudson River estuary, we used the following parameters: Type II and III areas (A) of 20 km^2, extending from the Narrows to the George Washington Bridge; an average sediment accumulation rate (SAR) of 4.5 cm year^{-1}, an average of sediment accumulation rates in Type II and Type III areas; a sediment bulk density (SBD) of 1 g cm^{-3} (based on our lab measurements); a sediment organic carbon content (TOC_{sed}) of 2–4 % (based on our lab measurements); and an organic carbon burial efficiency (SBE) of 100 % as there was no loss of organic carbon with depth in the sediment cores. This calculation indicated that the total organic carbon burial in the lower Hudson River estuary ranged from 1.8 to 3.6 $\times$ 10^{10} gC year^{-1}.

4.4 Carbon Burial in Estuarine Environments and its Global Implications

Previous studies on global carbon cycle have provided a variety of useful perspectives on organic carbon burial in different ocean regimes (Berner 1989; Hedges and Keil 1995; Schlunz and Schneider 2000). To investigate the amount of carbon burial in estuarine and deltaic environments worldwide, we have combined our results for the Yangtze and Hudson River estuaries with the results for other river-dominated estuaries in Table 1. Because the types of depositional environments for sediment accumulation and carbon burial in these 25 largest river-estuarine systems are unknown, we used a range of sediment carbon burial efficiencies (SBE) between 50 and 100 % to determine the potential range of total carbon buried in these river-estuarine systems. As indicated in Table 1, the 25 largest rivers in the world (in terms of sediment discharge) deliver $\sim6.5 \times 10^{15}$ g year^{-1} of sediments to their respective estuarine and coastal environments. If we assume a sediment organic carbon content of 1.75 %, based on the average of the high end of TOC_{sed} for the Yangtze River estuary (1.5 %) and the low end of TOC_{sed} for the Hudson River estuary (2 %), and use a range of 50 and 100 % for the sediment carbon burial efficiency, then the total carbon burial within these 25 largest river-estuarine systems would range from 6 to 11 $\times$ 10^{13} gC year^{-1}.

Globally, rivers discharge about $\sim2 \times 10^{16}$ g year^{-1} of fluvial sediment to the land–ocean interface (Meade 1996). The POC associated with this fluvial input has been estimated to be $\sim2.5 \times 10^{14}$ gC year^{-1}, which represents about half of the total organic carbon discharged by rivers (Meybeck 1982; Schlunz and Schneider 2000). Less than 5 % of the riverine particles delivered to the coastal margin reach the deep sea (Hedges 1992). This illustrates the effectiveness of the two-layer estuarine circulation pattern, which results in significant amounts of shelf sediment and carbon being transported landward during interglacial times and rapidly buried at the land–ocean interface, where the sediment surface is out of equilibrium with its physical regime (Olsen et al. 1993). The rapid accumulation of carbon-coated particles and the burial of organic carbon in these natural or human-impacted "non-equilibrium" areas removes TOC_{sed} from exposure to oxygenated surface water, captures it within the sedimentary environment by rapid deposition and burial, and causes low-energy areas at the land–ocean interface to be net sinks for atmospheric CO_2.

Table 1 Sediment discharge (10^6 mt year^{-1}) and organic carbon burial (10^{12} gC year^{-1}) in selected rivers worldwide

River	Sediment discharge[a] (10^6 mt year^{-1})	Sediment discharge rank	Organic carbon burial (10^{12} gC year^{-1})	References
Amazon, Brazil	1,150	1	4.5	Showers and Angle (1986)
Yellow, China	1,100	2	3.1–6.2[d]	Coynel et al. (2005)
Ganges–Brahmaputra, Bangladesh	1,050	3	7.2	Galy et al. (2007)
Yangtze, China (selected estuarine area)	480	4	1.6–4.9	This study
Yangtze, China (estuary + shelf)	480	4	7.4	Deng et al. (2006)
Irrawaddy, Burma	260	5	1.4–2.8[b,d]	Bird et al. (2008)
Magdalena, Colombia	220	6	ND[c]	
Mississippi, USA	210	7	2–4[d]	Bianchi et al. (2007)
Godavari, India	170	8	0.6	Balakrishna and Probst (2005)
Mekong, Vietnam	160	9	ND	
Red, Vietnam	160	9	ND	
Orinoco, Venezuela	150	11	1.7	Coynel et al. (2005)
Purari/Fly, New Guinea	110	12	0.52	Aller et al. (2008)
Mackenzie, Canada	100	13	2	Dittmar and Kattner (2003)
Parana/Uruguay, Brazil	100	13	ND	
Salween, Burma	100	13	1.4–2.8[b,d]	Bird et al. (2008)
Pearl, China	80	16	0.5	Ni et al. (2008)
Copper, USA	70	17	ND	
Choshui, Taiwan	66	18	0.25–0.5[d]	Goldsmith et al. (2008)
Yukon, USA	60	19	ND	
Amur, Russia	52	20	0.9	Nakatsuka et al. (2004)
Indus, Pakistan	50	21	ND	
Zaire, Zaire	43	22	2	Coynel et al. (2005)
Liao, China	41	23	ND	
Danube, Romania	40	24	ND	
Niger, Africa	40	25	ND	
Yenisey, Russia	5		0.17	Dittmar and Kattner (2003)
Lena, Russia	11		0.47	Dittmar and Kattner (2003)
Ob, Russia	16		0.31	Dittmar and Kattner (2003)
Hudson, USA	1.6		0.02–0.04	This study

[a] Data from Milliman and Meade (1983) and Meade (1996)

[b] Is an averaged value

[c] No data (ND)

[d] Organic carbon burial was calculated using the total riverine POC input and assuming a 50–100 % carbon burial efficiency

5 Conclusions

Within the global carbon cycle, it has been well established that remineralization of POC and DOC within the estuarine and shelf water column serves as a source for atmospheric CO_2. The importance of carbon burial in sediments at the land–ocean interface as a potential sink for atmospheric CO_2 has not been extensively addressed, because (1) the amount of organic carbon that is input to the system is derived from various sources, including riverine, marine, wastewater, and in situ productivity; (2) the amount of carbon buried at the land–ocean interface is spatially and temporally heterogeneous; and (3) estuaries and other systems at the land–ocean interface have been and continue to be significantly perturbed by urbanization and other human activities. Although each estuarine system (large or small) throughout the world has its own physical, chemical, biological, and geological features and processes, they are all characterized by a two-layer estuarine circulation pattern that promotes the landward transport, trapping, and accumulation of carbon-coated particles and POC at the land–ocean interface.

Our integrative results, spanning over 50 years, indicate that carbon is being rapidly buried in estuarine areas, where the sediment surface is currently out of equilibrium with its physical regime. These non-equilibrium areas can occur naturally, such as in the Yangtze River estuary, where vertical accretion of deltaic topset beds and horizontal progradation of foreset beds can be as high as 20 and 300 m year^{-1}, respectively. These non-equilibrium areas can also occur anthropogenically, such as in dredged-harbor areas within the Hudson River estuary, where the accumulation of carbon-rich sediments can be as high as 15–20 cm year^{-1}. The fine-grained and carbon-coated particles that escape estuarine systems are generally transported both *alongshore* on the shelf and *landward* into other protected low-energy coastal areas. For example, the fine-grained sediments escaping the Amazon River delta are generally transported northward and landward, forming muddy beaches and accumulating in protected coastal areas as far north as Venezuela (Smoak 2009). In addition, nutrient-rich estuarine water discharged onto the shelf can stimulate in situ production of POC, which sinks to the bottom and is transported landward back into estuaries or other coastal marginal areas.

Although carbon burial in the world's 25 largest river-estuarine–deltaic systems (~ 0.1 PgC year^{-1}) is small relative to the oceanic sink (~ 2 PgC year^{-1}) (Sabine et al. 2004), these 25 systems only account for a small areal component of the entire world's coastline. Future work involving a global network of estuarine and coastal scientists working in their own backyards may provide a platform for quantifying the extent of carbon burial along the entirety of the world's coastline. It is also important to determine whether carbon assimilation and accumulation in these areas have increased during the past 50 years in association with the increased loadings of agricultural and wastewater derived nutrients.

References

Aller RC, Blair NE, Brunskill GJ (2008) Early diagenetic cycling, incineration, and burial of sedimentary organic carbon in the central Gulf of Papua (Papua New Guinea). J Geophys Res 113:F01S09. doi:10.1029/2006JF000689

Balakrishna K, Probst JL (2005) Organic carbon transport and C/N ratio variations in a large tropical river: Godavari as a case study, India. Biogeochemistry 73(3):457–473

Benner R, Benitez-Nelson B, Kaiser K, Amon RMW (2004) Export of young terrigenous dissolved organic carbon from rivers to the Arctic Ocean. Geophys Res Lett 31:L05305. doi:10.1029/2003GL019251

Berner RA (1982) Burial of organic carbon and pyrite sulfur in the modern ocean: its geochemical and environmental significance. Am J Sci 282:451–473

Berner RA (1989) Biogeochemical cycles of carbon and sulfur and their effect on atmospheric oxygen over phanerozoic time. Palaeogeogr Palaeoclimatol Palaeoecol 75:97–122

Bianchi TS, Allison MA (2009) Large-river delta-front estuaries as natural "recorders" of global environmental change. Proc Natl Acad Sci USA 106(20):8085–8092

Bianchi TS, Wysocki LA, Stewart M, Filley TR, McKee BA (2007) Temporal variability in terrestrially-derived sources of particulate organic carbon in the lower Mississippi River and its upper tributaries. Geochim Cosmochim Acta 71:4425–4437

Bird MI, Robinson RAJ, Oo NW, Aye MM, Lu XX, Higgitt DL, Swe A, Tun T, Win SL, Aye KS, Win KMM, Hoey TB (2008) A preliminary estimate of organic carbon transport by the Ayeyarwady (Irrawaddy) and Thanlwin (Salween) Rivers of Myanmar. Quat Int 186:113–122

Biscaye PE (1994) Shelf edge exchange processes in the Southern Middel Atlantic Bight - SEEP - II. Deep Sea Res Part II Top Stud Oceanogr 41(2–3):229–230

Bokuniewicz HJ, Ellsworth JM (1986) Sediment budget for the Hudson system. Northeast Geol 8(3):9

Bolin B (1977) Changes of land biota and their importance for the carbon cycle. Science 196(4290):613–615

Bopp RF, Simpson HJ, Chillrud SN, Robinson DW (1993) Sediment-derived chronologies of persistent contaminants in Jamaica Bay, New-York. Estuaries 16(3B):608–616

Broecker WS (2003) Fossil fuel CO$_2$ and the angry climate beast. Eldigio Press, New York

Broecker WS, Takahashi T, Simpson HJ, Peng TH (1979) Fate of fossil fuel carbon dioxide and the global carbon budget. Science 206(4417):409–418

Cai WJ, Dai MH, Wang YC (2006) Air-sea exchange of carbon dioxide in ocean margins: a province-based synthesis. Geophys Res Lett 33(12):4

Canadell JG, Le Quere C, Raupach MR, Field CB, Buitenhuis ET, Ciais P, Conway TJ, Gillett NP, Houghton RA, Marland G (2007) Contributions to accelerating atmospheric CO2 growth from economic activity, carbon intensity, and efficiency of natural sinks. Proc Natl Acad Sci USA 104(47):18866–18870

Chillrud SN (1996) Transport and fate of particle associated contaminants in the Hudson River basin. Ph.D. Thesis, Columbia University, New York, NY, pp. 277

Coynel A, Seyler P, Etcheber H, Meybeck M, Orange D (2005) Spatial and seasonal dynamics of total suspended sediment and organic carbon species in the Congo River. Global Biogeochem Cycles 19(4):17

Deng B, Zhang J, Wu Y (2006) Recent sediment accumulation and carbon burial in the East China Sea. Glob Biogeochem Cycles 20:GB3014. doi:10.1029/2005GB002559

Dittmar T, Kattner G (2003) The biogeochemistry of the river and shelf ecosystem of the Arctic Ocean: a review. Mar Chem 83(3–4):103–120

Donoghue JF, Bricker OP, Olsen CR (1989) Particle-reactive radionuclides as tracers for sediment in the Susquehanna River and Chesapeake Bay. Estuar Coast Shelf Sci 29:341–360

Dürr HH, Laruelle GG, van Kempen CM, Slomp CP, Meybeck M, Middelkoop H (2011) World-wide typology of near-shore coastal systems: defining the estuarine filter of river inputs to the oceans. Estuar Coasts 34(3):441–458. doi:10.1007/s12237-011-9381-y

Eisma D (1998) Intertidal deposits: river mouths, tidal flats, and coastal lagoons, in CRC Marine Science Series. CRC Press, Boca Raton

Ellsworth JM (1986) Sources and sinks for fine-grained sediment in the lower Hudson River. Northeast Geol 8:141–155

Fagan KE, Mackenzie FT (2007) Air-sea CO2 exchange in a subtropical estuarine-coral reef system, Kaneohe Bay, Oahu, Hawaii. Mar Chem 106(1–2):174–191

Fairbridge RW (1961) Eustatic changes in sea level. Phys Chem Earth 4:99–185

Galy V, France-Lanord C, Beyssac O, Faure P, Kudrass H, Palhol F (2007) Efficient organic carbon burial in the Bengal fan sustained by the Himalayan erosional system. Nature 450:407–410

Geyer WR, Woodruff JD, Traykovski P (2001) Sediment transport and trapping in the Hudson River estuary. Estuaries 24(5):670–679

Goldsmith ST, Carey AE, Lyons WB, Kao SJ, Lee TY, Chen J (2008) Extreme storm events, landscape denudation, and carbon sequestration: Typhoon Mindulle, Choshui River, Taiwan. Geology 36(6):483–486

Green RE, Bianchi TS, Dagg MJ, Walker ND, Breed GA (2006) An organic carbon budget for the Mississippi River turbidity plume and plume contributions to air-sea CO_2 fluxes and bottom water hypoxia. Estuar Coasts 29(4):579–597

Hedges JI (1992) Global biogeochemical cycles—progress and problems. Mar Chem 39(1–3):67–93

Hedges JI, Keil RG (1995) Sedimentary organic matter preservation: an assessment and speculative synthesis. Mar Chem 49:81–115

Houghton RA, Goodale CL (2004) Effects of land-use change on the carbon balance of terrestrial ecosystems. In: DeFries RS, Asner GP, Houghton RA (eds) Ecosystems and land use change. American Geophysical Union, Washington, DC, pp 85–98

Klingbeil AD, Sommerfield CK (2005) Latest Holocene evolution and human disturbance of a channel segment in the Hudson River estuary. Mar Geol 218:135–153

Lu X, Zhai S, Niu L (2006) Sources and preservation of organic matter in recent sediment from the Changjiang (Yangtze River) estuary, China. Sci Mar 70(1):47–58

Mayer L (1994) Surface area control of organic carbon accumulation in continental shelf sediments. Geochim Cosmochim Acta 58(4):1271–1284

Mayer T, Johnson MG (1994) History of anthropogenic activities in Hamilton Harbor as determined from the sedimentary record. Environ Pollut 86(3):341–347

McKee BA, Aller RC, Allison MA, Bianchi TS, Kineke GC (2004) Transport and transformation of dissolved and particulate materials on continental margins influenced by major rivers: benthic boundary layer and seabed processes. Cont Shelf Res 24(7–8):899–926

Meade RH (1996) River-sediment inputs to major deltas. In: Milliman JD, Haq B (eds) Sea-level rise and coastal subsidence. Kluwer, London, pp 63–85

Meybeck M (1982) Carbon, nitrogen, and phosphorus transport by World Rivers. Am J Sci 282(4):401–450

Milliman JD, Meade RH (1983) World-wide delivery of river sediment to the oceans. J Geol 91(1):1–21

Mulholland PJ, Olsen CR (1992) Marine origin of Savannah River estuary sediments: evidence from radioactive and stable isotope tracers. Estuar Coast Shelf Sci 34(1):95–107

Nakatsuka T, Toda M, Kawamura K, Wakatsuchi M (2004) Dissolved and particulate organic carbon in the Sea of Okhotsk: transport from continental shelf to ocean interior. J Geophys Res 109:C09S14. doi:10.1029/2003JC001909

Ni HG, Lu FH, Luo XL, Tian HY, Zeng EY (2008) Riverine inputs of total organic carbon and suspended particulate matter from the Pearl River Delta to the coastal ocean off South China. Mar Pollut Bull 56(6):1150–1157

Olsen CR (1979) Radionuclides, sedimentation and the accumulation of pollutants in the Hudson estuary. Columbia University, New York, NY

Olsen CR, Cutshall NH, Larsen IL, Simpson HJ, Trier RM, Bopp RF (1984) An estuarine fine-particle budget determined from radionuclide tracers. Geo Mar Lett 4(3–4):157–160

Olsen CR, Thein M, Larsen IL, Lowry PD, Mulholland PJ, Cutshall NH, Byrd JT, Windom HL (1989) Plutonium, lead-210 and carbon isotopes in the Savannah estuary: riverborne versus marine sources. Environ Sci Technol 23(12):1475–1481

Olsen CR, Larsen IL, Mulholland PJ, Vondamm KL, Grebmeier JM, Schaffner LC, Diaz RJ, Nichols MM (1993) The concept of an equilibrium surface-applied to particle sources and contaminant distributions in estuarine sediments. Estuaries 16(3B):683–696

Panuzio FL (1965) Lower Hudson River siltation. In: Proceedings of the federal inter-agency sedimentation conference, 196. Miscellaneous Publ. No. 970, Agricultural Research Service, Jackson, Mississippi, pp. 512–550

Prentice IC, Farquhar GD, Fasham MJR, Goulden ML, Heimann M, Jaramillo VJ, Kheshgi HS, Quéré CL, Scholes RJ, Wallace DWR (2001) The carbon cycle and atmospheric carbon dioxide. In: Houghton JT, Ding Y, Griggs DJ, Noguer M, v. d. Linden PJ, Dai KMX, Johnson CA (eds) Climate change 2001: the scientific basis. Contribution of working group I to the third assessment report of the intergovernmental panel on climate change. Cambridge University Press, Cambridge, UK, and New York, NY, USA, pp 183–237

Sabine CL et al (2004) The oceanic sink for anthropogenic CO_2. Science 305(5682):367–371

Sanudo-Wilhelmy SA, Gill GA (1999) Impact of the clean water act on the levels of toxic metals in urban estuaries: the Hudson River estuary revisited. Environ Sci Technol 33(20):3477–3481

Schlunz B, Schneider RR (2000) Transport of terrestrial organic carbon to the oceans by rivers: re-estimating flux- and burial rates. Int J Earth Sci 88(4):599–606

Schubel JR (1968) Turbidity maximum of the northern Chesapeake Bay. Science 161:1013–1015

Schubel JR, Meade RH (1977) Man's impact on estuarine sedimentation. In: Estuarine pollution control and assessment, proceedings of a conference, vol 1. U.S. Gov. Print. Off, Washington, DC, pp 193–209

Sholkovitz ER (1976) Flocculation of dissolved organic and inorganic matter during the mixing of river water and seawater. Geochim Cosmochim Acta 40:831–845

Showers WJ, Angle DG (1986) Stable isotopic characterization of organic carbon accumulation on the Amazon continental shelf. Cont Shelf Res 6(1–2):227–244

Smith JP (2007) Short-to-medium term sediment accumulation in low-energy subtidal areas of lower Hudson River estuary: geochemical tracers and applications. Ph.D. Thesis, University of Massachusetts Boston, Boston, pp 212

Smoak JM (2009) Carbon, nitrogen and phosphorus mass balance for the amazon continental shelf. In: Liu KK et al. (eds) Carbon and nutrient fluxes in continental margins: a global synthesis. Springer, New York (in press)

Swanson RL, Bortman ML, O'Connor TP, Stanford HM (2004) Science, policy and the management of sewage materials: the New York City experience. Mar Pollut Bull 49:679–687

Wall GR, Nystrom EA, Litten S (2008) Suspended sediment transport in the freshwater reach of the Hudson River estuary in eastern New York. Estuar Coasts 31:542–553

Woodruff JD, Geyer WR, Sommerfield CK, Driscoll NW (2001) Seasonal variation of sediment deposition in the Hudson River estuary. Mar Geol 179(1–2):105–119

Wright LD (1989) Dispersal and deposition of river sediments in coastal seas: models from Asia and the tropics. Neth J Sea Res 23:493–500

Wu Y, Zhang J, Liu SM, Zhang ZF, Yao QZ, Hong GH, Cooper L (2007) Sources and distribution of carbon within the Yangtze River system. Estuar Coast Shelf Sci 71(1–2):13–25

Yang SL (1999) A study of coastal morphodynamics on the muddy islands in the Changjiang River estuary. J Coast Res 15(1):32–44

Yang SL, Ding PX, Zhu J, Zhao QY, Mao ZC (2000) Tidal flat morphodynamic processes of the Yangtze estuary and their engineering implications. China Ocean Eng 14(3):307–320

Yang SL, Ding PX, Chen SL (2001) Changes in progradation rate of the tidal flats at the mouth of the Changjiang (Yangtze) River, China. Geomorphology 38(1–2):167–180

Yang SL, Belkin IM, Belkina AI, Zhao QY, Zhu J, Ding P (2003) Delta response to decline in sediment supply from the Yangtze River: evidence of the recent four decades and expectations for the next half-century. Estuar Coast Shelf Sci 57(4):689–699

Yang SL, Shi Z, Zhao HY, Li P, Dai SB, Gao A (2004) Effects of human activities on the Yangtze River suspended sediment flux into the estuary in the last century. Hydrol Earth Syst Sci 8:1210–1216

Yang SL, Zhang J, Zhu J, Smith JP, Dai SB, Gao A, Li P (2005) Impact of dams on Yangtze River sediment supply to the sea and delta intertidal wetland response. J Geophys Res 110:F03006. doi:10.1029/2004JF000271

Zhu, J. (2003) Sediment accretion and erosion on tidal flats in the Yangtze River estuary and implications for future land reclamation. M.S. Thesis, East China Normal University, Shanghai, pp 103

Zhu J (2010) Geochemical and geospatial studies of sediment accumulation and carbon burial in the lower Hudson River estuary and its implications for the global carbon cycle. University of Massachusetts, Boston

Zhu J, Yang SL, Olsen CR (2006) Delta response to decline in sediment supply from the Yangtze River over the last 50 years and predictions for the future. Ocean Science Meeting Ocean Sci. Meet. Suppl., Honolulu, HI, pp OS16A-09

Zhu ZY, Zhang J, Wu Y, Lin J (2006b) Bulk particulate organic carbon in the East China Sea: tidal influence and bottom transport. Prog Oceanogr 69(1):37–60